Photosensitive quantum dot composites and their applications in optical structures

Lin Pang,[a] Kevin Tetz, Yaoming Shen, Chyong-Hua Chen, and Yeshaiahu Fainman
Department of Electrical and Computer Engineering, University of California, San Diego, 9500 Gilman Drive, La Jolla, California 92093-0407

(Received 17 February 2005; accepted 19 September 2005; published 3 November 2005)

Commercially available CdSe/ZnS and PbSe colloidal semiconductor quantum dots were employed to produce both an electron beam sensitive poly(methyl methacrylate) (PMMA)-quantum-dot (QD) positive composite via a prepolymerization processing and an electron beam and ultraviolet (UV) light sensitive SU-8-QD negative composite via a direct dispersion procedure. Compared to the QDs in the original colloidal solutions, the photoluminescence of the composites shifts to shorter wavelength due to the oxidation of the surfaces of the QDs. Using the QD composites, optical integrated circuits such as grating and waveguide structures were fabricated by direct electron beam writing and UV optical lithography. The characterization results show promising applications in optoelectronics for the QD composites. © *2005 American Vacuum Society.*
[DOI: 10.1116/1.2122867]

I. INTRODUCTION

In recent years, semiconductor quantum dots (QDs) have attracted much interest due to their properties of nanoscale quantum confinement that possess great promise for numerous optoelectronics and photonics applications including communications,[1,2] displays,[3] and biology.[4] While there are many possible fabrication methods, semiconductor QDs formed in colloidal solution via chemical synthesis have been shown to be a promising route to QD realization.[5–7] In colloidal solutions, however, QDs are suspended in a solvent, making them less practical for fabrication and integration of photonic and optoelectronic devices. The introduction of such QDs into a solid-state matrix, therefore, is of great interest for numerous applications. One approach incorporates the QDs into polymer thin films and has shown great promise.[3,8] The incorporation of QDs into a thick, bulk polymer matrix has also been investigated by using many complicated synthesis techniques to prevent aggregation of QDs during the polymerization process when QDs were dissolved in vinyl monomers and processed to a radical polymerization.[9–12] We have described a simple method using the prepolymerization of monomers to prevent the QDs from separating from the polymer matrix.[13] Most importantly, the sensitivity of this composite to electron beams makes it attractive in the fabrication of photonic devices.

In this article, after summarizing the prepolymerization method and presenting results of fabricating poly(methyl methacrylate) (PMMA)–QD composites with different sizes of CdSe/ZnS and PbSe colloidal QDs, we will describe a method for fabricating QD composite optical waveguide structures. Furthermore, a different polymer–QD composite, SU-8–QD composite, was made by carefully dispersing QDs into a SU-8 matrix. Photoluminescence and patterning of these composites proved that the diffusion of the QDs into the polymer matrices not only maintained the optical properties of the QDs, but also preserved the photosensitivity of the polymer matrices to the electron beams and ultraviolet (UV) light. The PMMA–QD composite synthetic procedure and the applications of fabricating photonic devices are described in Sec. II. Section III discusses the SU-8–QD composite and its application of fabricating composite optical waveguides. The conclusion is given in Sec. IV.

II. PMMA–QD BULK ELECTRON BEAM SENSITIVE COMPOSITE

A. PMMA–QD composite

The synthesis of the PMMA–QD composite processing is based on the radical polymerization of methyl methacrylate (MMA). Under vigorous stirring, a quantity of nanoparticle colloidal solution of quantum dots in toluene (Evident Technologies) was slowly added into the distilled MMA with a concentration of radical initiator azobisisobutyronitrile of 0.1% in weight. It is commonly known that the uniform dispersion of nanoparticles in the polymer–QD composites is hampered by separation and cluster aggregation from the matrix. Direct polymerization exhibited serious nonuniformity and clustering of the QDs.[13] Figure 1 shows the scanning electron microscope (SEM) photograph of QD agglomeration resulting from direct polymerization, in which the MMA–QD solution was placed into a thermostatic water bath at 60 °C for about 20 h. If the MMA–QD solution was, however, first placed into a thermostatic water bath at 90 °C for about 20 min for a short and quick polymerization, or prepolymerization, and then was transferred into an oven at 60 °C to completely polymerize for 20 h, the aggregation did not happen.[13] PMMA–QD composites with 620 nm CdSe/ZnS core-shell quantum dots (maple red–orange) are shown in Fig. 2(a), while 500 nm CdSe/ZnS core-shell (spearmint green) and 1550 nm PbSe (mocha) quantum dot composites are shown in Fig. 2(b). Figures 2(a) and 2(b)

[a]Electronic mail: lpang@ece.ucsd.edu

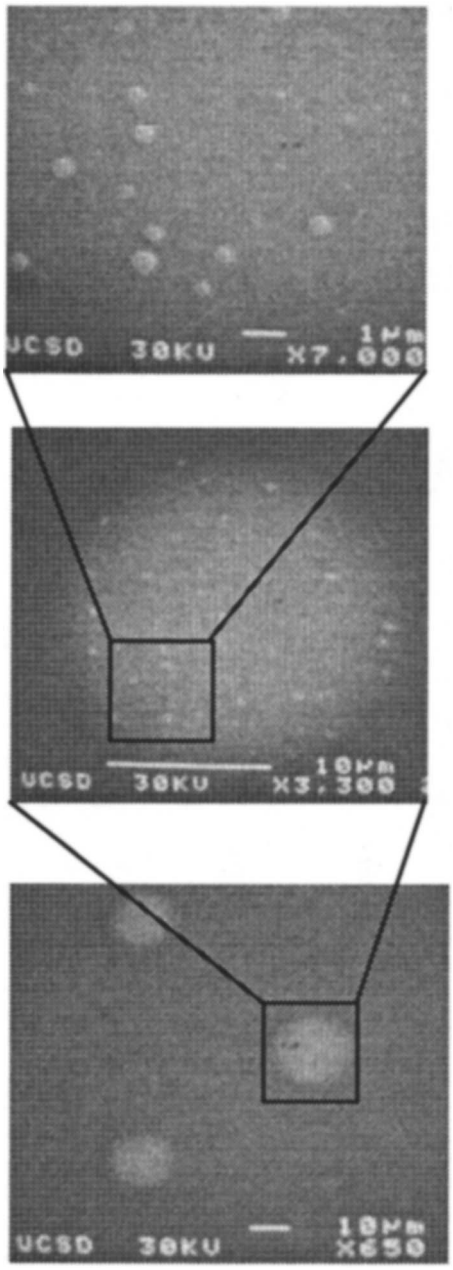

FIG. 1. SEM photographs of clusters of quantum dots in the PMMA–QD composite by direct polymerization.

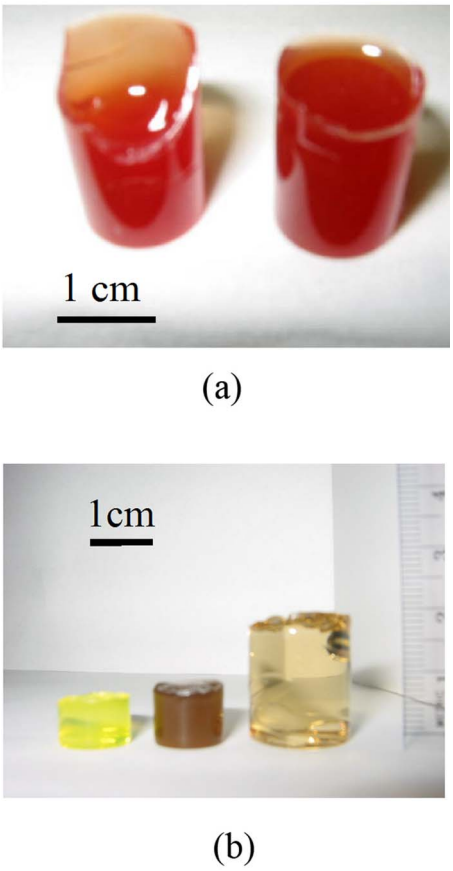

FIG. 2. Photographs of the PMMA–QD composites by the prepolymerization: (a) with 620 nm CdSe/ZnS quantum dots in concentration of 0.6 mg/ml; (b) from left to right, 500 nm CdSe/ZnS in concentration of 0.13 mg/ml, 1550 nm PbSe quantum dots in concentration of 0.5 mg/ml and 0.14 mg/ml.

were taken by a digital camera in the ambient environment to show the qualities of the composites. The color is uniform over the entirety of the samples with no observable defects. The elimination of aggregation of the QDs lies in the rapid polymerization of couples of MMA monomers to form oligomers, which envelope the QDs and prevent them from aggregating during the following postpolymerization process.[13]

Because their emission wavelength peak is approximately at the wavelength of a He–Ne laser, we will focus on the PMMA–QD composites with 620 nm CdSe/ZnS quantum dots in the following investigation. An argon laser with a wavelength of 488 nm was used to pump the QD composites. A monochromator (CVI DK480) and a GaAs photocounter (Hamamatsu H7421-50) were used to measure the photoluminescence (PL) of the composites. Figure 3 shows the PL spectra of both the QDs in toluene solution (right) and in a PMMA–QD composite slide (left) of 1 mm thick. The composite slide was produced by casting the prepolymerized QD–polymer (0.6 mg/ml) into a chamber made from glass slides. The PL peak of the solid PMMA–QD composite matrix occurs at about 617 nm with full-width half maximum (FWHM) of about 19 nm, whereas the PL peak for the QDs in toluene solution of concentration 2.5 mg/ml is at 625 nm with the FWHM of about 16 nm.

B. Electron-beam positive PMMA–QD composite

By exploiting the nature of the sensitivity of PMMA to an electron beam, our PMMA–QD composites may also be used for direct writing electron beam lithography to make nanostructures. This fabrication approach is very attractive for numerous applications of QD composites. For the proof-of-concept experiment, the prepolymerized PMMA–QD composite was dispersed in MMA and then spin coated on a Si substrate. After the soft baking step, the PMMA–QD layer was patterned by *e*-beam lithography in a modified SEM

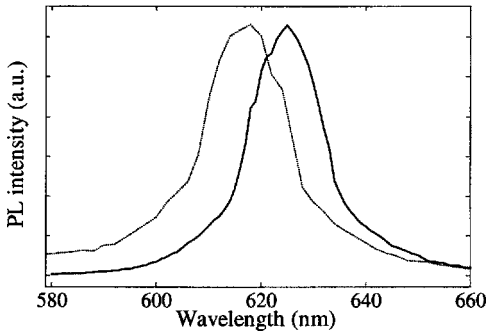

FIG. 3. PL spectra of QDs in toluene solution (solid line-right) and in the PMMA–QD composite (dash line-left).

(JEOL JSM-6400), followed by development in solution of methyl isobutyl ketone (MIBK) and isopropyl alcohol (IPA) in the ratio of MIBK:IPA=1:2. Figure 4 shows a SEM photograph of a structure with a 1.5 μm period with feature sizes of 200 and 300 nm.

The grating structure shown in Fig. 4 demonstrates that, after adding QDs into a PMMA resist, the PMMA–QD composite is still sensitive to electron beam exposure. This sensitivity, however, is reduced dramatically. For the grating structure shown in Fig. 4, the exposure dosage was about 210 μC/cm^2. Compared to the same structure achieved by the PMMA resist at a dosage of about 170 μC/cm^2 within the same development time of about 60 s, the dosage needed for the PMMA–QD composite increased approximately 40 μC/cm^2. As for the resolution of the PMMA–QD composite, we have no evidence to show the resolution limit as far as our *e*-beam writing system is concerned. With the PMMA resist at an acceleration voltage of 35 kV, the smallest structures obtainable with our modified SEM system were a 50 nm hole in diameter and an 80 nm line. We have obtained the same structures in the PMMA–QD composite by increasing the exposure dosage or prolonging the development time. For example, the exposure dosage was about 5 μC/cm^2 for the 50 nm hole in PMMA–QD resist, whereas it was 3.3 μC/cm^2 for PMMA resist. Nevertheless, when the features approach the sizes of the QDs, i.e., several nanometers, by using higher acceleration voltage,[14] the QDs will likely have a significant influence on the resolution of the PMMA–QD composite. Although the organic matrix is not as environmentally stable as semiconductor QD structures fabricated via molecular beam epitaxy and metalorganic chemical vapor deposition techniques, its flexibility and compatibility with organic optoelectronics make it a very attractive candidate for many applications.

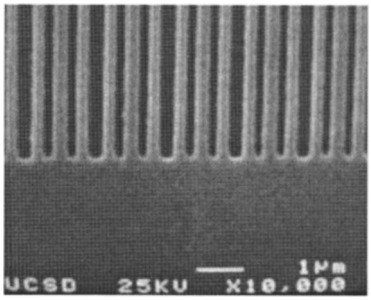

FIG. 4. SEM photograph of a PMMA–QD composite structure by directly writing the composite with electron beams.

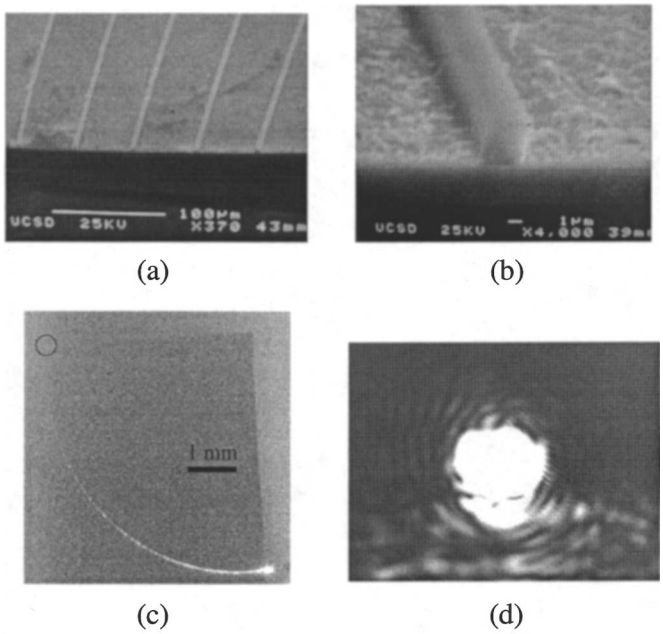

FIG. 5. (a) SEM photograph of a PMMA–QD composite waveguide array on a SiO_2/Si substrate. (b) Closeup of PMMA–QD composite waveguide with thickness of 3.5 μm and width of 2.5 μm. (c) Image of optical beam trace traveling along the waveguide. (d) Mode profile from the waveguide output.

C. PMMA–QD composite waveguide structure

e-beam lithography is not a suitable process for the fabrication of microdevices, such as optical waveguides, with the PMMA–QD composites. High doses and large exposed areas are required because PMMA is a positive resist and possesses low sensitivity to electron beams. As an alternative, optical lithography and dry etching are utilized to make PMMA–QD composite waveguides. We used anisole as a solvent to spin coat a 3.5 μm thick PMMA–QD composite layer on a substrate of SiO_2/Si (7 μm/600 μm). After a 20 min soft bake in an oven at 170 °C, a 1 μm thick BPRS-100 positive resist was spin coated on top of the PMMA–QD layer. Baked at 110 °C for 30 min, the resist layer was exposed by a suitable mask in a mask aligner and developed in PLSI developer (trisodium phosphate and sodium matasilicate in water) of PLSI:H_2O=1:3. A 20 nm thick Au layer was evaporated on top of the resist pattern. Using a liftoff process, an Au waveguide pattern was achieved. Finally, reactive ion etching was used to transfer the pattern into the PMMA–QD composite at a power of 150 W with an oxygen flow of 8 sccm as shown in Fig. 5. Figure 5(a) shows an array of waveguides, and Fig. 5(b) is a closeup image of one of the waveguides, which shows a rectangular profile of the 3.5 μm thick and 2.5 μm wide waveguide cross section. There is a significant residue remaining in the etched area

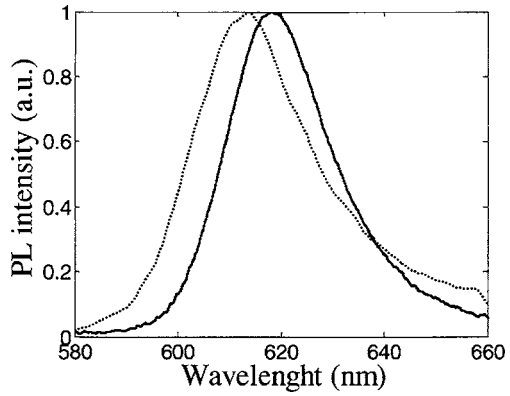

FIG. 6. PL spectra of QDs in SU-8 solution (solid line-right) and in solid SU-8 composite film (dash line-left).

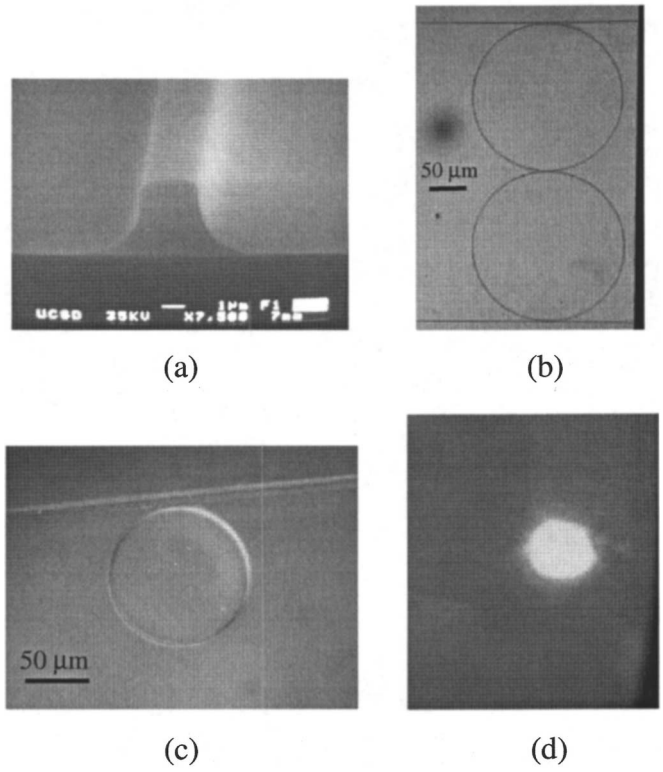

FIG. 7. SU-8 composite structures by using *e*-beam lithography: (a) SEM photograph of the cross section of a SU-8 composite waveguide with a height of 3.5 μm and a width of 2.5 μm in the upper portion and 6 μm in the lower portion; (b) microscopic image of waveguide and microring cavity with the ring diameter of about 200 μm; (c) microscopic image of waveguide and microdisk cavity with the disk diameter of about 100 μm; and (d) a single-mode profile from a waveguide output.

due to incomplete etching. Also, rough stripes can be seen on the sidewall, which come from the roughness of the mask edges. The rough sidewall produced light scattering when a light traveled in the waveguide as shown in Fig. 5(c). Figure 5(c) is a top-view image taken by a charge coupled device (CCD) camera (TM-7EX, Pulnix) through a microscope on top of the waveguide sample, in which a light beam of about 635 nm from a laser diode was coupled into the waveguide through fiber-to-waveguide coupling. The dark area in Fig. 5(c) indicates the substrate of the device, and the bright spot in the lower right-hand corner indicates the coupling location from the fiber to the input of the waveguide. A spot in a circle in the upper left-hand corner denotes the output of the guided beam. The scattering light is contributed to the rough surfaces of the waveguide. The profile of the guided mode is shown in Fig. 5(d). The mode profile was taken along the beam propagating direction by imaging the waveguide output onto a CCD by a 20× microscopic objective lens and a lens of 100 mm focal length. The multimode profile shown in Fig. 5(d) matches the prediction of the mode calculation by considering the waveguide size, material index, and the coupled wavelength.

III. ELECTRON BEAM AND UV LIGHT SENSITIVE SU-8–QD COMPOSITE

A. SU-8–QD composite

The resist SU-8 has been used as an UV sensitive material in microelectromechanical systems[15] and in holographic lithography.[16,17] It also has been demonstrated to be an appropriate material for fabrication of polymer waveguides and microring structures by using *e*-beam lithography,[18] although its resolution is inferior to PMMA. If a SU-8–QD composite can be achieved, the sensitivity of the SU-8 material to electron beam and UV light will make it very easy to produce high-quality (less rough) quantum-dot composite single-mode-waveguide structures to investigate the QD properties in waveguide structures.

Because of the incompatibility of SU-8 with toluene, which is the solvent of the QD colloid, the QDs first must be transferred into a SU-8 compatible solvent, such as hexane or propylene ether acetate, etc., then added into the SU-8 solution very slowly with strong stirring. Precautions must be taken to prevent clustering of the QDs. Compared with the aforementioned PMMA–QD composite, the QD concentration in the SU-8–QD composite cannot be increased arbitrarily high due to the lesser dispersibility of QDs in the viscous SU-8–polymer solution.

SU-8–QD composite was prepared by spin coating the solution onto a substrate followed by a soft bake in a 90 °C oven for 5 min. The PL in the SU-8–QD composites was measured as shown in Fig. 6 with the same setup as in Sec. II A. The quantum dots used to make the SU-8 composite are from a different batch bought from the same company. Their central emission wavelength was slightly different from the one used in making the PMMA–QD composite. However, the trend of the PL after the solidification is the same. The PL blueshifts from 618 nm in liquid SU-8 solution to 613.5 nm in SU-8 solid film. Similarly, the FWHM increases from 24 nm in solution to 27 nm after being dried. A blueshift of QD in the PL spectra had been reported for different kinds of quantum dots when exposed in air (oxygen).[19,20] For our case, the blueshift could also be attributed to the oxidation of the QDs' surface.

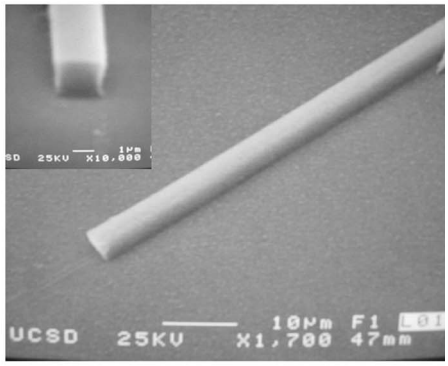

(a)

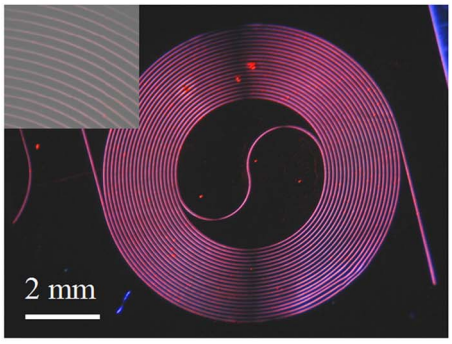

(b)

FIG. 8. SU-8 composite structures by using KalSUSS mask aligner: (a) SEM photographs of a straight waveguide and (b) microscopic images of a spiral waveguide excited with a UV laser (364 nm).

B. SU-8–QD composite waveguides

SU-8 is a chemically amplified negative UV and electron beam resist. The acid generated during the exposure catalyzes the crosslinking at postexposure bake (PEB),[16] which means that less exposure dosages are needed compared to other resists. Figure 7(a) shows a SEM image of an *e*-beam exposed SU-8 composite waveguide with a height of 3.5 μm and a width of 2.5 μm in the upper portion. Although a smooth sidewall was achieved, the waveguide does not have a rectangular profile. The bottom portion of the waveguide extended to 6 μm due to the scattering of the electrons from the surface of the SiO_2 underlayer. The conductivity could be improved by employing a conductive layer on the top and even on the bottom of the SU-8 layer. In order to show the whole waveguide structure, we used a microscope to take photographs as shown in Figs. 7(b) and 7(c). Figure 7(b) shows a microscopic photograph of a waveguide–ring coupler with the ring diameter of about 200 μm. Figure 7(c) is a waveguide–disk coupler with the disk diameter of about 100 μm. Figure 7(d) is a guided mode profile by imaging the waveguide output onto a near-infrared CCD camera (Merlin, Indigo) through a 20× microscopic objective lens and a imaging lens while coupling a 1.55 μm laser beam from a fiber to a L-shape SU-8 waveguide. The single mode profile, as shown in Fig. 7(d), matches the design of the waveguide structure.

As we know, SU-8 resist is very sensitive to electron beams, usually 0.8 $\mu C/cm^2$ is typical for a SU-8 waveguide writing followed by PEB on a hotplate at 95 °C for 1 min. However, for the SU-8–QD composite, the exposure needs to be increased to over 2 $\mu C/cm^2$ for the same PEB processing as a result of the influence of the quantum dots component in the SU-8 matrix.

Due to the limitation of the positioning stage in our SEM writing system, the maximal writing area is about 3×3 mm^2. For the larger area waveguide structures, optical lithography is a good alternative, and dry etching is unnecessary. After exposure through a mask, the SU-8–QD composite layer on the SiO_2/Si substrate was baked on a hotplate for the PEB step, developed in propylene glycol methyl ether acetate. Figure 8(a) shows the SEM photograph of the fabricated waveguide with smooth sidewalls with width of 2.1 μm and height of 1.7 μm shown in the inset. Figure 8(b) shows a spiral waveguide with a total length of 1 m and 4 mm internal diameter, and 8 mm external diameter, respectively. The interval between the waveguides is 50 μm. We observed the whole spiral waveguide structure using a 0.7× microscope, in which we had enough space to introduce a UV light (364 nm from Ar^+ laser) to illuminate the sample area to stimulate the quantum dots. We can clearly see the photoluminescence from the emission of the CdSe/ZnS quantum dots in the SU-8 composite waveguide. The two dark areas on the spiral waveguide were due to the shade of the UV illumination. The large bright spots in the spiral areas are the QD clusters in the composite, which can be removed by filtering the SU-8–QD solution before spin coating. The inset in Fig. 8(b) shows the uniform photoluminescence of the waveguides.

IV. CONCLUSION

We have presented approaches to fabricate an electron beam sensitive PMMA–quantum dot positive composite via prepolymerization, and an electron beam and UV sensitive SU-8–QD negative composite via direct dispersion using commercially available colloidal semiconductor QDs. Investigations of patterning these composites via electron beam lithography and optical lithography demonstrated a promising application of these composites in photonics. By using these materials, waveguide structures have been fabricated, and preliminary experiments have been performed, which show promising results. An optical amplifier using composite optical waveguides is being designed, and a nonlinear optical phase shift[21] is also being considered using the composite photonic devices.

ACKNOWLEDGMENTS

This study was supported in part by the National Science Foundation and the Defense Advanced Research Projects Agency.

[1]L. Jacak, P. Hawrylak, and A. Wojs, *Quantum Dots* (Springer, Berlin, Germany, 1998).
[2]V. I. Klimov, A. A. Mikhailovsky, S. Xu, A. Malko, J. A. Hollingsworth, C. A. Leatherdale, H.-J. Eisler, and M. G. Bawendi, Science **290**, 314 (2000).
[3]V. Colvin, M. Schlamp, and A. Alivisatos, Nature (London) **370**, 354 (1994).
[4]M. Bruchez, M. Moronne, P. Gin, S. Weiss, and A. P. Alivisatos, Science **281**, 2013 (1998).
[5]Y. Wang, A. Suna, W. Mahler, and R. Kasowski, J. Chem. Phys. **87**, 7315 (1987).
[6]C. B. Murray, D. J. Norris, and M. G. Bawendi, J. Am. Chem. Soc. **115**, 8706 (1993).
[7]M. A. Hines and P. Guyot-Sionnest, J. Phys. Chem. **100**, 468 (1996).
[8]M. C. Schlamp, X. G. Peng, and A. P. Alivisatos, J. Appl. Phys. **82**, 5837 (1997).
[9]M.-Y. Gao, Y. Yang, B. Yang, F.-L. Bian, and J.-C. Shen, Chem. Commun. 2779 (1994).
[10]D. E. Fogg, L. H. Radzilowski, R. Blanski, R. R. Schrock, and E. L. Thomas, Macromolecules **30**, 417 (1997).
[11]J. Lee, V. C. Sundar, J. R. Heine, M. G. Bawendi, and K. F. Jensen, Adv. Mater. (Weinheim, Ger.) **12**, 1102 (2000).
[12]H. Zhang, Z. Cui, Y. Wang, K. Zhang, X. Ji, C. Lu, B. Yang, and M. Gao, Adv. Mater. (Weinheim, Ger.) **15**, 777 (2003).
[13]L. Pang, Y.-M. Shen, K. Tetz, and Y. Fainman, Opt. Express **13**, 44 (2005).
[14]W. Chen and H. Ahmed, Appl. Phys. Lett. **63**, 1116 (1993).
[15]H. Lorenz, M. Despont, N. Fahrni, J. Brugger, P. Renaud, and P. Vettiger, Sens. Actuators, A **64**, 33 (1998).
[16]L. Pang, W. Nakagawa, and Y. Fainman, Opt. Eng. **42**, 2912 (2003).
[17]L. Pang, W. Nakagawa, and Y. Fainman, Appl. Opt. **42**, 5450 (2003).
[18]G. T. Paloczi, Y. Huang, A. Yariv, and S. Mookherjea, Opt. Express **11**, 2666 (2003).
[19]W. G. J. H. M. van Sark, P. L. T. M. Frederix, D. J. Van den Heuvel, H. C. Gerritsen, A. A. Bol, J. N. J. van Lingen, C. de Mello Donega, and A. Meijerink, J. Phys. Chem. B **105**, 8281 (2001).
[20]M. Jones, J. Nedeljkovic, R. J. Ellingson, A. J. Nozik, and G. Rumbles, J. Phys. Chem. B **107**, 11346 (2003).
[21]H. Nakamura *et al.*, Opt. Express **12**, 6606 (2004).